Microfluid Nanofluid (2013) 15:49–55
DOI 10.1007/s10404-012-1126-0

RESEARCH PAPER

Magnetic concentration of particles and cells in ferrofluid flow through a straight microchannel using attracting magnets

Jian Zeng · Chen Chen · Pallavi Vedantam · Tzuen-Rong Tzeng · Xiangchun Xuan

Received: 20 September 2012 / Accepted: 6 December 2012 / Published online: 20 December 2012

Abstract Concentrating particles to a detectable level is often necessary in many applications. Although magnetic force has long been used to enrich magnetic (or magnetically tagged) particles in suspensions, magnetic concentration of diamagnetic particles is relatively new and little reported. We demonstrate in this work a simple magnetic technique to concentrate polystyrene particles and live yeast cells in ferrofluid flow through a straight rectangular microchannel using negative magnetophoresis. The magnetic field gradient is created by two attracting permanent magnets that are placed on the top and bottom of the planar microfluidic device and held in position by their natural attractive force. The magnet–magnet distance is mainly controlled by the thickness of the device substrate and can be made small, allowing for the use of a dilute ferrofluid in the developed magnetic concentration technique. This advantage not only enables a magnetic/fluorescent label-free handling of diamagnetic particles, but also renders such handling biocompatible.

Keywords Microfluidics · Ferrofluid · Particle concentration · Magnetophoresis · Lab on a chip

J. Zeng · C. Chen · X. Xuan (✉)
Department of Mechanical Engineering, Clemson University, Clemson, SC 29634-0921, USA
e-mail: xcxuan@clemson.edu

P. Vedantam · T.-R. Tzeng
Department of Biological Sciences, Clemson University, Clemson, SC 29634-0314, USA

1 Introduction

Concentrating particles to a detectable level is often necessary and critical in many applications such as environment monitoring, food safety, and water quality control (Nilsson et al. 2009; Pratt et al. 2011). In microfluidic devices, particles can be concentrated by means of contact or contactless methods (Johann 2006). Contact methods include the use of chemical, mechanical and physical processes for particle immobilization or blocking (Ghubade et al. 2009; Hamblin et al. 2010; Zheng et al. 2011). This type of methods allows for straightforward handling, but often suffers from irreversible particle adhesions. Contactless methods utilize an externally applied or internally induced force field, such as electric (Church et al. 2010; Jen and Chen 2009; Lapizco-Encinas et al. 2004, 2005; Lapizco-Encinas and Rito-Palmomares 2007; Lewpiriyawong et al. 2012; Ohta et al. 2007; Sabounchi et al. 2008; Shafiee et al. 2009), optical (Kumar et al. 2010; Zhang et al. 2012), acoustic (Shi et al. 2009; Hammarström et al. 2010), and thermal (Duhr and Braun 2005) forces, to trap and enrich particles in suspensions. These methods allow for the concentration of particles while the force field is on and the release of the trapped particles by simply turning the field off. They, however, often require complex preparations, intricate microchannel designs, and expensive equipment.

Magnetic force has long been used to concentrate magnetic (or magnetically tagged) particles through positive magnetophoresis, where the particles are attracted along the magnetic field gradient towards the magnetic field source (Afshar et al. 2011a, b; Bronzeau and Pamme 2008; Gijs 2004; Gijs et al. 2010; Liu et al. 2009; Nguyen 2012; Pamme 2006, 2012; Ramadan and Gijs 2012). Like other contact methods, the trapped magnetic particles tend

to form chains or clusters and cannot be completely removed from a surface even after the external magnetic field has been removed. Magnetic concentration of diamagnetic (often called nonmagnetic by non-physicists) particles has been demonstrated in both paramagnetic solutions and ferrofluids using negative magnetophoresis. The magnetic field gradient is created by the use of two repulsing (Fateen 2002; Feinstein and Prentiss 2006; Winkleman et al. 2004) or attracting (Peyman et al. 2009) magnets, where the particles are concentrated in between and outside the aligned magnets, respectively. The involving magnets need to be fixed using a special mechanical setup and have been implemented to work with micro capillaries only. In addition, diamagnetic particles can be concentrated in ferrofluids using patterned soft magnets or electromagnets (Halverson et al. 2006; Erb and Yellen 2008; Kose et al. 2009; Kose and Koser 2012), which, however, both require complicated device fabrications.

This work develops a simple magnetic technique to concentrate diamagnetic particles in ferrofluid flow through a straight rectangular microchannel using attracting permanent magnets. The two magnets are placed on the top and bottom of the planar microfluidic device and held in position by their natural attractive force, which eliminates the use of a special mechanical setup or specially designed magnets. Moreover, as the magnet–magnet distance can be made small by reducing the microchannel substrate thickness, a dilute ferrofluid is sufficient to implement a continuous magnetic concentration of both 5-μm polystyrene particles and live yeast cells.

2 Experimental technique

The straight microchannel was fabricated using the standard soft lithography method and formed by bonding a polydimethylsiloxane (PDMS) slab with a glass cover slip (Fisher Scientific., 0.17–0.25 mm thick). It is 2 cm long and has a rectangular shape with a uniform width of 550 μm and a uniform depth of 60 μm. The detailed procedure for the microchannel fabrication is referred to Zeng et al. (2012). Two attracting Neodymium–Iron–Boron (NdFeB) permanent magnets (B421, 1/4″ × 1/8″ × 1/16″, K&J Magnetics Inc.) are placed above the PDMS slab and underneath the cover slip, respectively. Their separating distance can be controlled by varying the thickness of the PDMS slab. Figure 1 shows a picture of the microfluidic device used in the particle/cell concentration experiments, where the inlet reservoir was formed by inserting a 1 ml pipette tip into the through hole in the PDMS slab.

The particle solution was made by suspending 5-μm polystyrene particles (Duke Scientific Corp.) in 0.05 × EMG

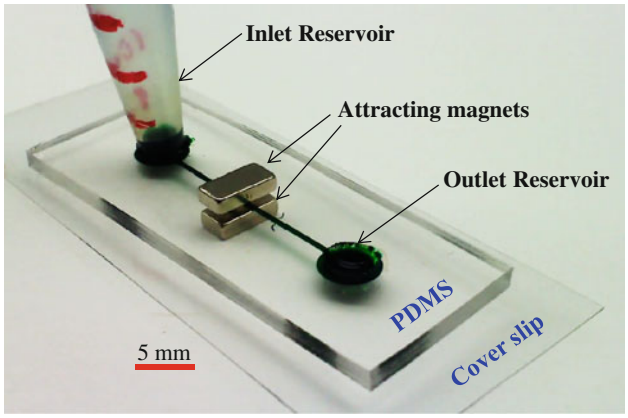

Fig. 1 Picture of the microfluidic device (the microchannel and reservoirs are filled with *green* food dye for clarity) used in the experiment

408 ferrofluid (Ferrotec Corp.) to a concentration of 5×10^6 particles/ml. The dilute ferrofluid was prepared by mixing the original EMG 408 ferrofluid with pure water at a volume ratio of 1:19. Yeast cells (*Saccharomyces cerevisiae*) were cultured overnight in Sabouraud's dextrose broth in a shaker incubator at 30 °C, and were re-suspended in sterile phosphate buffered saline (PBS) solution to a concentration of 5.73×10^8 cells/ml. Before use, live yeast cells were washed with de-ionized water three times and re-suspended in 0.05 × EMG 408 ferrofluid to a final concentration of around 5×10^6 cells/ml. The measured diameter of yeast cells is 5 μm on average. Tween 20 (Fisher Scientific) was added to both the particle and cell suspensions at 0.1 % by volume to minimize their aggregations and adhesions to microchannel walls.

The particle or cell suspension in the diluted ferrofluid was introduced only to the inlet reservoir (see Fig. 1). The liquid height in the inlet reservoir was varied to achieve different ferrofluid flow speeds. The outlet reservoir was emptied prior to experiment. To minimize the back-flow effects due to liquid build-up during the course of particle/cell concentration, the outlet reservoir was intentionally made large. Particle/cell motion was visualized using an inverted microscope (Nikon Eclipse TE2000U, Nikon Instruments, Lewisville, TX) under a bright-field illumination. Digital videos (at a time rate of around 12 frames per seconds) and images were recorded through a CCD camera (Nikon DS-Qi1Mc) and post-processed using the Nikon imaging software (NIS-Elements AR 2.30).

3 Magnetic concentration mechanism

Diamagnetic particles undergo negative magnetophoresis in a ferrofluid when subjected to a non-uniform magnetic field. This motion, $\mathbf{U}_m$, points in the direction of decreasing

magnetic field and is expressed as (Liang et al. 2011; Liang and Xuan 2012),

$$\mathbf{U}_m = \frac{-\mu_0 \phi a^2}{9\eta f_D} \frac{M_d L(\alpha) \nabla \mathbf{H}^2}{H} \quad (1)$$

$$L(\alpha) = \coth(\alpha) - \frac{1}{\alpha} \text{ and } \alpha = \frac{\pi \mu_0 M_d H d^3}{6 k_B T} \quad (2)$$

where μ_0 is the permeability of free space, ϕ is the volume fraction of magnetic nanoparticles in the ferrofluid, a is the radius of diamagnetic particles, η is the ferrofluid viscosity, f_D is the drag coefficient to account for the particle–wall interactions (Liang et al. 2011; Vojtisek et al. 2012; Zhu et al. 2011a, b, 2012a), M_d is the saturation moment of magnetic nanoparticles, $L(\alpha)$ represents Langevin function (Rosensweig 1979), $\mathbf{H}$ is the magnetic field with a magnitude of H, d is the average diameter of magnetic nanoparticles, k_B is the Boltzmann constant, and T is the ferrofluid temperature. Note that in Eq. (1), the contribution from the magnetization of diamagnetic particles has been neglected because it is nearly 4 orders of magnitude smaller than that from the diluted ferrofluid we used in experiments (Gijs 2004, 2010; Pamme 2006). Apparently, the magnetophoretic velocity, $\mathbf{U}_m$, increases for larger diamagnetic particles in a ferrofluid with a greater volume fraction of magnetic nanoparticles.

The use of two attracting magnets of equal geometry and magnetization in Fig. 1 can confine the majority of the magnetic field lines in between the two polar surfaces. This in turn creates strong magnetic gradients within the microchannel at near the front and rear edges of the magnets as evidenced by the magnetic field contour (the darker color, the larger magnitude) in Fig. 2. The magnetic field distribution was obtained by superimposing the magnetic fields of the two magnets (Zeng et al. 2012), which was each computed from Furlani's analytical formula (Furlani 2001) as stated in our earlier work (Liang et al. 2011) and is thus skipped here for brevity. Note that the ferrofluid effects on magnetic field are neglected in this analytical formula, which has been proved reasonable in recent studies (Liang et al. 2011; Zeng et al. 2012; Zhu et al. 2011a, b, 2012b). As indicated by the arrow plots in Fig. 2, the induced magnetophoretic velocity, $\mathbf{U}_m$, of diamagnetic particles is against the pressure-driven flow velocity of the suspending ferrofluid, $\mathbf{U}_f$. Therefore, particles will be stagnated at the locations where the two velocities are counterbalanced, leading to a continuous trapping and concentration of particles. Such a magnetic concentration works more effectively for larger diamagnetic particles in a ferrofluid with a higher volume fraction of magnetic nanoparticles. In addition, since $\mathbf{U}_m$ is nearly uniform across the microchannel while $\mathbf{U}_f$ has a parabolic profile (see the vector plots of these two velocities in Fig. 2), particles travelling along different flow paths should be stagnated at dissimilar locations. Specifically, particles travelling near the channel walls can be trapped further away from the magnet than those near the channel center. The interactions between the fluid and particles are hypothesized to cause a pair of counter-rotating circulations of the trapped particles as schematically illustrated in Fig. 2 (see the curved arrows for circulating directions).

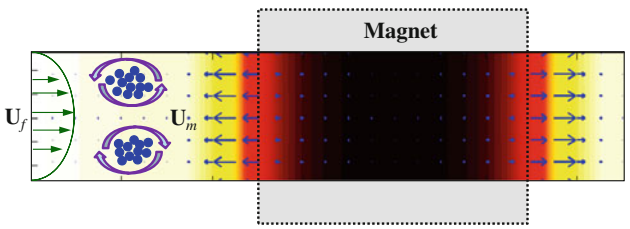

Fig. 2 Illustration of the mechanism for magnetic concentration of diamagnetic particles in a pressure-driven ferrofluid flow through a straight microchannel with two attracting magnets. The *background color* indicates the magnetic field contour (the *darker color*, the larger magnitude). The *thin arrows* display the velocity vectors of ferrofluid flow, $\mathbf{U}_f$, particle magnetophoresis, $\mathbf{U}_m$. Particles are trapped in the locations where $\mathbf{U}_m$ can counterbalance $\mathbf{U}_f$. The *curved arrows* indicate the hypothesized circulating directions of the trapped diamagnetic particles; see the text for the explanation

4 Results and discussion

4.1 Magnetic concentration of polystyrene particles

Figure 3 shows the top-view images of 5-μm polystyrene particles during magnetic concentration at the leading edge of the two attracting magnets with respect to the ferrofluid flow. Allowing for the experiment to run, these snapshots were obtained under a continuous bright-field illumination at 5 min increments, starting with the initial time of 5 s. It is important to note that fluorescent labeling of particles is usually required for visualization purposes of particles suspended in concentrated ferrofluids (Liang et al. 2011; Zeng et al. 2012; Zhu et al. 2010, 2011a, b, 2012b). This is, however, not necessary in our experiment due to the diluted state of the ferrofluid. The magnet–magnet distance is 2.2 mm, including the 2-mm-thick PDMS and the 200-μm-thick cover slip. The average flow speed is 2 mm/s, at which very few particles (<5 % in number) were observed to escape from the downstream side of the magnets. It was estimated through theoretical calculation based on the measured liquid height difference in the inlet and outlet reservoirs (Zeng et al. 2012; Zhu et al. 2012a), and also verified by tracking individual particles in the inlet section of the microchannel that is distant from the magnets.

As predicted in the mechanism section (see Sect. 3), polystyrene particles are continuously concentrated in the ferrofluid flow by negative magnetophoresis (see Fig. 2; Zeng et al. 2012) in front of the leading edge of the attracting magnets. However, wave-like chaotic motions are observed for the trapped particles, which is evident in Fig. 3 [see images in (b) and (c)]. This is beyond our expectation considering the fact of low-Reynolds number (computed as 0.2) for the tested flow. We speculate that it may be a consequence of the misaligned magnets that can take place in two circumstances: one is that the two magnets themselves are not aligned with their centers being slightly shifted, and the other is that either or both of the two magnets are not placed symmetrically with respect to the microchannel. If neither of these misalignments occurs, diamagnetic particles can be magnetically concentrated in two symmetrically distributed circulations relative to the channel centerline (cf. Fig. 5). In addition, one can see from Fig. 3 that the particle trapping zone is extended further to upstream when more and more particles are accumulated. This may be simply because particles need to take a larger space for further accumulations.

We investigated the magnet–magnet distance effects on the magnetic concentration of 5-μm polystyrene particles by varying the thickness of the PDMS slab. The maximum average flow speed of 0.05 × EMG 408 ferrofluid, at which the magnetic concentration of all flowing particles can still be achieved, was measured for three values of PDMS thickness (1, 2, and 5 mm). Also recorded were the minimum ferrofluid flow speeds at which no particles can be trapped for various PDMS thicknesses. A line graph of these two relationships is presented in Fig. 4a, which, as expected, demonstrates an increasing flow speed (and hence a greater particle throughput) at a smaller magnet–magnet distance for both circumstances. More importantly, Fig. 4a can work as a phase diagram for diamagnetic particle concentration, where the two lines divide the diagram into three distinct regions, i.e., complete trapping, partial trapping and zero trapping. Figure 4b1–b3 illustrates the snapshot images of the concentrated particles 10 min after the running of the experiment for each of the three PDMS thicknesses. An apparently greater trapping zone is observed for a larger magnet–magnet distance. This may be attributed to the reduced effect of confining magnetic field lines in between two magnets with a larger separation gap, and so the magnetic field gradients can extend to a farther distance outside of the magnets.

We also studied the flow rate effects on diamagnetic particle concentration by decreasing the ferrofluid flow speed from the above-determined maximum value for the case with a 2-mm thick PDMS. It was found that the flow effect on the location of particle trapping zone is insignificant. This may be because the magnetophoretic particle velocity decays very quickly from the edge of the magnets, which is clearly indicated by the arrow plots in Fig. 2. However, the number of trapped particles decreases at a smaller ferrofluid speed within the same amount of concentration time because less particles travel into the channel with the flow.

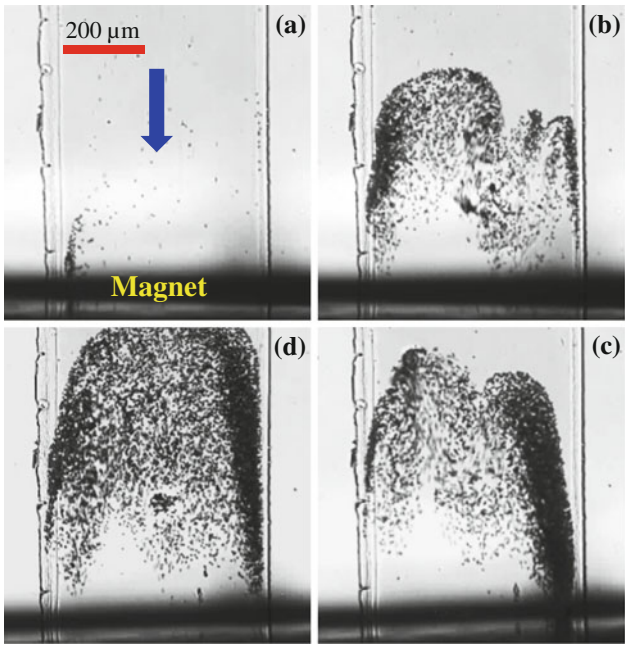

Fig. 3 Snapshot images demonstrating the development of magnetic concentration of 5 μm polystyrene particles in 0.05 × EMG 408 ferrofluid flow after 5 s (**a**), 5 min (**b**), 10 min (**c**), and 15 min (**d**). The magnet–magnet distance is 2.2 mm and the average flow speed is 2 mm/s. The *block arrow* in **a** indicates the flow direction

4.2 Magnetic concentration of live yeast cells

Figure 5 shows a snapshot image of live yeast cells after 10 min of continuous concentration in 0.05 × EMG 408 ferrofluid. The microfluidic device is similar to that used in Fig. 3 with a magnet–magnet distance of 2.2 mm. The magnetic concentration was implemented at an average ferrofluid flow speed of 2 mm/s, which is identical to that for concentrating 5-μm polystyrene particles in the same device. This is reasonable considering that the live yeast cells we used have an average diameter of 5 μm. However, distinct from the wave-like dynamic motions for the trapped particles in Fig. 3, yeast cells appear to be accumulated inside two nearly symmetric circulations as demonstrated in Fig. 5. As noted above, we attribute the latter phenomenon to the precise alignment of the two attracting magnets with respect to each other and to the microchannel as well. However, the circulating directions of the trapped yeast cells in Fig. 5 (see the curved arrows) are opposite to our hypothesized directions in Fig. 2. The reason behind this is

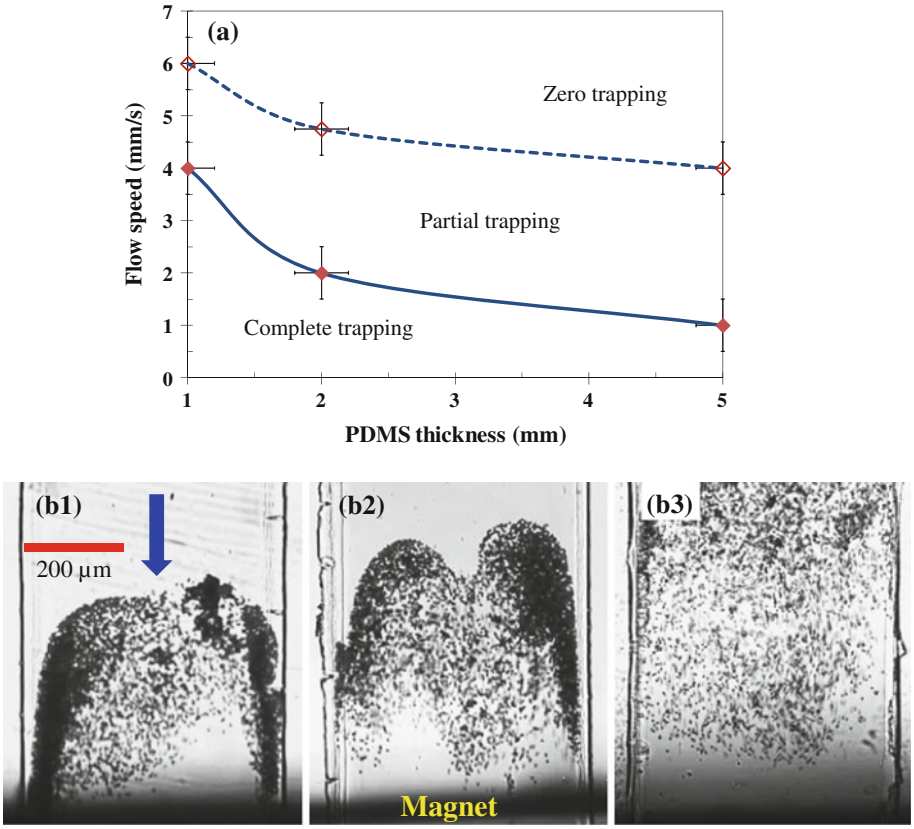

Fig. 4 **a** Phase diagram illustrating the magnet–magnet distance (controlled by the thickness of the PDMS slab) effect on the magnetic concentration (reflected by the flow speed) of 5 µm polystyrene particles in 0.05 × EMG 408 ferrofluid. The *two lines* represent the measured ferrofluid flow speeds at which all (*solid line* with *filled symbols*) and no (*dashed line* with *hollow symbols*) particles can be trapped, respectively. *Error bars* are included for experimental data (*symbols*). The *lines* are used only for guiding the eyes. **b** *Snapshot images* of concentrated particles (each was taken 10 min after the experiment started) for the three tested magnet–magnet distances. The *block arrow* in (**b1**) indicates the flow direction

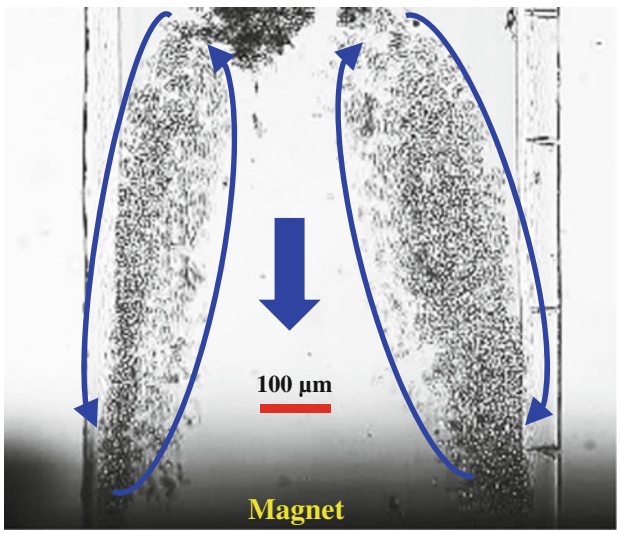

Fig. 5 *Snapshot image* of magnetically concentrated yeast cells in 0.05 × EMG 408 ferrofluid. The average flow speed is 2 mm/s and the magnet–magnet distance is 2.2 mm, which is identical to those in Fig. 3 for 5-µm polystyrene particles. The *curved arrows* highlight the two nearly symmetric circulations in which yeast cells are magnetically trapped and enriched. The *block arrow* indicates the flow direction of the ferrofluid suspension through the microchannel

currently unclear, which needs a further investigation that considers the complex cell–fluid interactions. The two magnets could be easily removed during the experiment, after which the concentrated particles and cells were observed to be washed out by the ferrofluid flow easily.

A biocompatibility test was conducted by comparing the ratio of live to dead yeast cells before and after the experiment using a spread plate. The detail is referred to our earlier work (Zeng et al. 2012). In brief, 100 µl of the diluted cell suspension was plated in triplicates on potato dextrose agar plates. After cell incubation at 30 °C for 24–48 h, the colonies were counted and the CFU/ml (colony forming unit) was determined. A slight decrease (around 5 %) in the cell count was observed, which indicates that the exposure to dilute ferrofluid and magnetic force has negligible influences on the viability of yeast cells. Further experiments will be done to test the biocompatibility of this ferrofluid-based magnetic concentration approach with vulnerable cells like mammalian cells.

5 Conclusions

We have developed a simple technique for magnetic concentration of diamagnetic particles in ferrofluid flow through a straight microchannel using two attracting magnets. As they are placed on the top and bottom of the microfluidic device and held in position by the natural attractive force, these magnets can be readily removed during and after experiments. Moreover, using a glass

cover slip and a thin layer of PDMS to decrease the magnet–magnet distance, the suspending ferrofluid can be significantly diluted and so bright-field illumination is sufficient for particle visualization. Such a magnetic/fluorescent label-free particle handling technique has been demonstrated by concentrating both 5-μm polystyrene particles and live yeast cells in 0.05 × EMG 408 ferrofluid. The effects of ferrofluid flow speed and magnet–magnet distance on the concentration performance are examined for polystyrene particles. Distinct flow patterns have been observed for concentrated particles, which are speculated to be associated with the alignment of the two attracting magnets. The evidence of the magnetic concentration of yeast cells without significant biological harm proves that it can be useful for bio applications where bioparticle enrichment is required. We are currently developing a numerical model with the aim of simulating the observed diamagnetic particle/cell trapping behaviors in ferrofluid microflows.

Acknowledgments This work was supported by NSF under grant CBET-1150670 (Xuan) and by Clemson University through the University Research Grant (Xuan and Tzeng).

References

Afshar R, Moser Y, Lehnert T, Gijs MAM (2011a) Magnetic particle dosing and size separation in a microfluidic channel. Sens Actuat B 154:73–80

Afshar R, Moser Y, Lehnert T, Gijs MAM (2011b) Three-dimensional magnetic focusing of superparamagnetic beads for on-chip agglutination assays. Anal Chem 83:1022–1029

Bronzeau S, Pamme N (2008) Simultaneous bioassays in a microfluidic channel on plugs of different magnetic particles. Analytica Chim Acta 609:105–112

Church C, Zhu J, Huang G, Tzeng TR, Xuan X (2010) Integrated electrical concentration and lysis of cells in a microfluidic chip. Biomicrofluid 4:044101

Duhr S, Braun D (2005) Two-dimensional colloidal crystals formed by thermophoresis and convection. Appl Phys Lett 86:131921

Erb RM, Yellen BB (2008) Concentration gradients in mixed magnetic and nonmagnetic colloidal suspensions. J Appl Phys 103:07A312

Fateen SK (2002) Magnetophoretic focusing of submicron particles dispersed in a polymer-stabilized magnetic fluid. MIT, PhD dissertation

Feinstein E, Prentiss M (2006) Three-dimensional self-assembly of structures using the pressure due to a ferrofluid in a magnetic field gradient. J Appl Phys 99:064901

Furlani EP (2001) Permanent magnet and electromechanical devices: materials, analysis, and applications. Academic Press, London

Ghubade A, Mandal S, Chaudhury R, Singh RK, Bhattacharya S (2009) Dielectrophoresis assisted concentration of micro-particles and their rapid quantitation based on optical means. Biomed Microdev 11:987–995

Gijs MAM (2004) Magnetic bead handling on-chip: new opportunities for analytical applications. Microfluid Nanofluid 1:22–40

Gijs MAM, Lacharme F, Lehmann U (2010) Microfluidic applications of magnetic particles for biological analysis and catalysis. Chem Rev 110:1518–1563

Halverson D, Kalghatgi S, Yellen B, Friedman G (2006) Manipulation of nonmagnetic nanobeads in dilute ferrofluid. J Appl Phys 99:08P504

Hamblin MN, Xuan J, Maynes D, Tolley HD, Belnap DM, Woolley AT, Lee M, Hawkins AR (2010) Selective trapping and concentration of nanoparticles and viruses in dual-height nanofluidic channels. Lab Chip 10:173–178

Hammarström B, Evander M, Barbeau H, Bruzelius M, Larsson J, Laurell T, Nilsson J (2010) Non-contact acoustic cell trapping in disposable glass capillaries. Lab Chip 10:2251–2257

Jen CP, Chen TW (2009) Selective trapping of live and dead mammalian cells using insulator-based dielectrophoresis within open-top microstructures. Biomed Microdev 11:597–607

Johann RM (2006) Cell trapping in microfluidic chips. Anal Bioanal Chem 385:408–412

Kose AR, Koser A (2012) Ferrofluid mediated nanocytometry. Lab Chip 12:190–196

Kose AR, Fischer B, Mao L, Koser H (2009) Label-free cellular manipulation and sorting via biocompatible ferrofluids. Proc Natl Acad Sci USA 106(51):21478–21483

Kumar A, Kwon JS, Williams SJ, Green NG, Yip NK, Wereley ST (2010) Optically modulated electrokinetic manipulation and concentration of colloidal particles near an electrode surface. Langmuir 26:5262–5272

Lapizco-Encinas BH, Rito-Palmomares M (2007) Dielectrophoresis for the manipulation of nanobioparticles. Electrophoresis 28:4521–4538

Lapizco-Encinas BH, Simmons BA, Cummings EB, Fintschenko Y (2004) Dielectrophoretic concentration and separation of live and dead bacteria in an array of insulators. Anal Chem 76:1571–1579

Lapizco-Encinas BH, Davalos RV, Simmons BA, Cummings EB, Fintschenko Y (2005) An insulator-based (electrodeless) dielectrophoretic concentrator for microbes in water. J Microbiol Methods 62:317–326

Lewpiriyawong N, Yang C, Lam YC (2012) Electrokinetically driven concentration of particles and cells by dielectrophoresis with DC-offset AC electric field. Microfluid Nanofluid 12:723–733

Liang L, Xuan X (2012) Diamagnetic particle focusing in ferromicrofluidics using a single magnet. Microfluid Nanofluid 13:637–643

Liang L, Zhu J, Xuan X (2011) Three-dimensional diamagnetic particle deflection in ferrofluid microchannel flows. Biomicrofluid 5:034110

Liu CX, Stakenborg T, Peeters S, Lagae L (2009) Cell manipulation with magnetic particles toward microfluidic cytometry. J Appl Phys 105:102011–102014

Nguyen NT (2012) Micro-magnetofluidics: interactions between magnetism and fluid flow on the microscale. Microfluid Nanofluid 12:1–16

Nilsson J, Evander M, Hammarstrom B, Laurell T (2009) Review of cell and particle trapping in microfluidic systems. Anal Chimica Acta 649:141–157

Ohta AT, Chiou PY, Wu MC (2007) Dynamic microparticle control via optoelectronic tweezers. J Microelectromech Sys 16:491–499

Pamme N (2006) Magnetism and microfluidics. Lab Chip 6:24–38

Pamme N (2012) On-chip bioanalysis with magnetic particles. Current Opinion Chem Biology 16:436–443

Peyman SA, Kwan EY, Margarson O, Iles A, Pamme N (2009) Diamagnetic repulsion-A versatile tool for label-free particle handling in microfluidic devices. J Chromatography A 1216:9055–9062

Pratt ED, Huang C, Hawkins BG, Gleghorn JP, Kirby BJ (2011) Rare cell capture in microfluidic devices. Chem Engineering Sci 66:1508–1522

Ramadan Q, Gijs MAM (2012) Microfluidic applications of functionalized magnetic particles for environmental analysis: focus on waterborne pathogen detection. Microfluid Nanofluid 13:529–542

Rosensweig RE (1979) Fluid Dynamics and Science of Magnetic Liquids. Adv Electronics Electron Phys 48:103–199

Sabounchi P, Morales AM, Ponce P, Lee LP, Simmons BA, Davalos RV (2008) Sample concentration and impedance detection on a microfluidic polymer chip. Biomed Microdev 10:661–670

Shafiee H, Caldwell JL, Sano MB, Davalos RD (2009) Contactless dielectrophoresis: a new technique for cell manipulation. Biomed Microdev 11:997–1006

Shi J, Mao X, Lin SS, Huang TJ (2009) Acoustic tweezers: patterning cells and microparticles using standing surface acoustic waves (SSAW). Lab Chip 9:2890–2895

Vojtisek M, Tarn MD, Hirota N, Pamme N (2012) Microfluidic devices in superconducting magnets: on-chip free-flow diamagnetophoresis of polymer particles and bubbles. Microfluid Nanofluid 13:625–635

Winkleman A, Gudiksen KL, Ryan D, Whitesides GM (2004) A magnetic trap for living cells suspended in a paramagnetic buffer. Appl Phys Lett 85:2411–2413

Zeng J, Chen C, Vedantam P, Brown V, Tzeng TR, Xuan X (2012) Three-dimensional magnetic focusing of particles and cells in ferrofluid flow through a straight microchannel. J Micromech Microeng 22:105018

Zhang Y, Lei H, Li Y, Li B (2012) Microbe removal using a micrometre-sized optical fiber. Lab Chip 12:1302–1308

Zheng S, Lin HK, Lu B, Williams A, Datar R, Cote RJ, Tai YC (2011) 3D microfilter device for viable circulating tumor cell (CTC) enrichment from blood. Biomed Microdev 13:203–213

Zhu T, Marrero F, Mao LD (2010) Continuous separation of non-magnetic particles inside ferrofluids. Microfluid Nanofluid 9:1003–1009

Zhu T, Cheng R, Mao L (2011a) Focusing microparticles in a microchannel with ferrofluids. Microfluid Nanofluid 11:695–701

Zhu T, Lichlyter DJ, Haidekker MA, Mao L (2011b) Analytical model of microfluidic transport of non-magnetic particles in ferrofluids under the influence of a permanent magnet. Microfluid Nanofluid 10:1233–1245

Zhu J, Liang L, Xuan X (2012a) On-chip manipulation of nonmagnetic particles in paramagnetic solutions using embedded permanent magnets. Microfluid Nanofluid 12:65–73

Zhu T, Cheng R, Lee SA, Rajaraman E, Eiteman MA, Querec TD, Unger ER, Mao L (2012b) Continuous-flow ferrohydrodynamic sorting of particles and cells in microfluidic devices. Microfluid Nanofluid 14:645–654